Lorentzian Quantum Gravity and the Graviton Spectral Function

Jannik Fehre,[1] Daniel F. Litim,[2] Jan M. Pawlowski,[1,3] and Manuel Reichert[2]

[1]*Institut für Theoretische Physik, Universität Heidelberg, Philosophenweg 16, 69120 Heidelberg, Germany*
[2]*Department of Physics and Astronomy, University of Sussex, Brighton BN1 9QH, United Kingdom*
[3]*ExtreMe Matter Institute EMMI, GSI Helmholtzzentrum für Schwerionenforschung mbH, Planckstrasse 1, 64291 Darmstadt, Germany*

We present the first direct and nonperturbative computation of the graviton spectral function in quantum gravity. This is achieved with the help of a novel Lorentzian renormalization group approach, combined with a spectral representation of correlation functions. We find a positive graviton spectral function, showing a massless one-graviton peak and a multigraviton continuum with an asymptotically safe scaling for large spectral values. We also study the impact of a cosmological constant. Further steps to investigate scattering processes and unitarity in asymptotically safe quantum gravity are indicated.

Introduction.—The quest for a consistent quantum theory of gravity continues to offer challenges [1]. An important contender is asymptotically safe gravity [2], where the metric field remains the fundamental carrier of the gravitational force. In this purely quantum field theoretical setup the trans-Planckian ultraviolet regime of quantum gravity is governed by an *interacting* fixed point, and gravity is ruled by the same principles as the standard model of particle physics.

The field of asymptotically safe gravity has seen substantial progress in the past decades, mostly using Euclidean functional renormalization [3], for reviews see [4–13]. Nevertheless, the question of unitarity is far from being settled [11,14], as many results are obtained within Euclidean signature. Naturally, the Wick rotation—already a subtle issue on flat Minkowski spacetimes—is further complicated by the dynamical metric. Still, first steps towards computations with Lorentzian signature have been reported [15–25], also for other quantum gravity approaches [26–32].

In this work, we put forward the first *bona fide* Lorentzian renormalization group study of asymptotically safe gravity. The key idea is the use of spectral representations for correlation functions, together with an expansion about flat Minkowski spacetime [13]. In particular, propagators obey the Källén-Lehmann (KL) representation [33,34]. This allows us to find the gravitational fixed point in Lorentzian signature alongside the graviton spectral function. Most notably, the existence of the latter offers access to the graviton propagator for general complex momenta, including timelike momenta relevant for graviton-mediated scattering processes.

Lorentzian quantum gravity and spectral functions.—We consider Lorentzian quantum gravity based on the classical Einstein-Hilbert action

$$S_{\text{EH}}[g_{\mu\nu}] = \frac{1}{16\pi G_N} \int d^4x |\det g_{\mu\nu}|^{\frac{1}{2}} (\mathcal{R} - 2\Lambda), \quad (1)$$

with Newton's constant G_N, cosmological constant Λ, and Ricci scalar $\mathcal{R}[g_{\mu\nu}]$, augmented with a gauge-fixing and ghost action. We use a flat Minkowskian background $\eta = \text{diag}(1, -1)$ and split the metric field $g_{\mu\nu} = \eta_{\mu\nu} + \sqrt{16\pi G_N} h_{\mu\nu}$ linearly into background and fluctuation $h_{\mu\nu}$. The main object of interest in the present work is the spectral function of the transverse-traceless (TT) graviton mode with the scalar coefficient $\mathcal{G}_{hh}$, for which we assume the existence of a KL representation. It relates the spectral function to the propagator via

$$\mathcal{G}_{hh}(p_0, |\vec{p}|) = \int_0^\infty \frac{d\lambda}{\pi} \frac{\lambda \rho_h(\lambda, |\vec{p}|)}{\lambda^2 + p_0^2}, \quad (2)$$

with the temporal and spatial momentum p_0 and $\vec{p}$, respectively, the spectral values λ, and the graviton spectral function

$$\rho_h(\lambda, |\vec{p}|) = \lim_{\varepsilon \to 0} 2\text{Im}\mathcal{G}_{hh}(p_0 = -i(\lambda + i\varepsilon), |\vec{p}|). \quad (3)$$

The spectral function acts as a linear response function of the two-point correlator, encoding the energy spectrum of the theory. For asymptotic states, it can be understood as a probability density for the transition to an excited state with energy λ. The existence of a spectral representation cannot

be taken for granted; but if it exists, it tightly constrains the analytic structure of the propagator and the asymptotes of the spectral function, see [35,36] for a discussion in Yang-Mills theories.

It is convenient to parameterize the spectral function at $\vec{p} = 0$ through a single-graviton delta peak with mass m_h and a multigraviton continuum f_h starting out at the threshold $\lambda = 2m_h$,

$$\rho_h(\lambda) = \frac{1}{Z_h}[2\pi\delta(\lambda^2 - m_h^2) + \theta(\lambda^2 - 4m_h^2)f_h(\lambda)]. \quad (4)$$

Classically, the spectral function is given by a single graviton peak with $m_h = 0$ and a trivial wave-function renormalization, $Z_h = 1$. Quantum fluctuations change the value of Z_h and lead to a multigraviton continuum f_h. For small spectral values, f_h approaches a finite value which can be determined using perturbation theory in an effective theory below the Planck scale. For spectral values approaching the Planck scale and above, the spectral function becomes sensitive to the ultraviolet (UV) completion and nonperturbative techniques are required for its determination.

Spectral renormalization group.—To establish the existence of Eq. (4), we set up a functional renormalization group (FRG) approach for Lorentzian quantum field theories, utilizing the spectral functional framework developed in [36,37]. This approach is based on a modified dispersion $p^2 \to p^2 + R_k(p^2)$, where we use the Lorentz-invariant choice

$$R_k = Z_\phi k^2. \quad (5)$$

This is a Callan-Symanzik (CS) cutoff including the on-shell wave-function renormalization Z_ϕ of the fluctuation fields $\phi = (h_{\mu\nu}, c_\mu, \bar{c}_\mu)$. The cutoff Eq. (5) shifts the on-shell condition by k^2 to larger values without introducing poles or cuts into the propagator. Conversely, using a standard momentum-dependent Lorentz-invariant regulator $R_k(p^2)$ necessarily introduces poles and cuts in the complex plane. Then, Eq. (2) does not hold at finite k. Hence, for the present study, we use Eq. (5) which does not spoil Eq. (2) from the outset.

While the cutoff Eq. (5) is best suited to extract spectral data, it comes at a price: the corresponding FRG flow requires additional renormalization because the standard UV divergences and counterterms resurface [38]. In practice, local divergences of the flow must be absorbed in the parameters of the cutoff-dependent effective action. Here, we use dimensional regularization, which respects the symmetries of the theory including gauge and diffeomorphism invariance, see [36,37]. This leads to a well-defined finite flow for effective actions Γ_k with Euclidean or Lorentzian signature,

$$\partial_t \Gamma_k^{(hh)} = -\frac{1}{2} \bigotimes + \bigotimes - 2 \bigotimes - \partial_t S_{\text{ct},k}^{(hh)}$$

FIG. 1. Flow of the graviton two-point function. Double (dotted) lines represent graviton (ghosts) propagators, dots indicate vertices, and the cross denotes a regulator insertion.

$$\partial_t \Gamma_k[\phi] = \frac{1}{2}\text{Tr}\mathcal{G}_k[\phi]\partial_t \mathcal{R}_k - \partial_t S_{\text{ct},k}[\phi]. \quad (6)$$

Here, $\mathcal{R}_k$ is the regulator matrix of all graviton and ghost modes. Similarly, $\mathcal{G}_k[\phi] = 1/(\Gamma_k^{(2)}[\phi] + \mathcal{R}_k)$ with $\Gamma_k^{(2)} \equiv \delta^2\Gamma_k/\delta\phi\delta\phi$ is the field-dependent propagator matrix at scale k, and we have introduced the "RG time" parameter $t = \ln k/k_{\text{ref}}$ with a reference scale k_{ref}.

The spectral flow Eq. (6) can be derived from the standard finite Wetterich flow [39] with spatial-momentum regulators $R_k(\vec{p}^2) \to Z_\phi k^2$ as briefly outlined in the Supplemental Material [40], see also [54]. Spatial-momentum regulators also preserve the spectral representation but break Lorentz invariance. The latter is restored in the above limit, in which also the counterterms $\partial_t S_{\text{ct},k}$ emerge naturally in a well-defined limit of finite flows.

With Eq. (6), we can provide explicit flow equations for the graviton propagator or vertices. For example, the flow for the graviton two-point function follows from Eq. (6) through a vertex expansion of $\Gamma_k[\phi]$ about vanishing fluctuation field $\phi = 0$. It is extracted from the graviton TT mode whose scalar propagator reads $\mathcal{G}_{hh} = (\Gamma_{\text{TT}}^{(hh)} + R_k)^{-1}$, with

$$\Gamma_{\text{TT}}^{(hh)}(p) = Z_h(p)(p^2 + \mu k^2). \quad (7)$$

Here, $Z_h(p)$ is the momentum-dependent graviton wave function, and μ the on-shell graviton mass parameter. With this parametrization, the graviton propagator has a pole at $m_h^2 = k^2(1 + \mu)$, cf., the delta peak in the spectral function Eq. (4). The wave-function renormalization in Eqs. (4) and (5) is defined on-shell $Z_h \equiv Z_h(p^2 = -m_h^2)$, the Lorentzian signature being key for this definition.

Schematically, the nonperturbative flow for the graviton two-point function is displayed in Fig. 1. Apart from regulator insertions and prefactors, it resembles one-loop diagrams, though with nonperturbative propagators and vertices. We further need the flow of gravitational vertices, in particular the three-graviton vertex. Here, we limit ourselves to vertices at vanishing momentum, where we may exploit equations derived in Euclidean signature as these fall back onto their Lorentzian counterparts required here [55,56]. Differences in the technical setup are subleading as long as the mass parameter stays away from off-shell poles, and the graviton anomalous dimension $\eta_h = -\partial_t \ln Z_h$ remains small.

Flow of the graviton spectral function.—We are now ready to provide an explicit nonperturbative flow for the

graviton spectral function Eq. (4). Using the flow for the graviton propagator with Eqs. (2) and (3), we find

$$\partial_t \rho_h = -2\mathrm{Im}\mathcal{G}_{hh}^2(\partial_t \Gamma_{\mathrm{TT}}^{(hh)} + \partial_t R_k), \qquad (8)$$

where the right-hand side is evaluated at $p = -i(\lambda + i\varepsilon)$, and the present spectral approach allows us to take this limit analytically, see [36,37]. Using the spectral representation Eq. (2) for gravitons and ghosts, all diagrams in Fig. 1 are now expressed as integrals over spectral values and a dimensionally regularized loop momentum. This reads

$$\partial_t \Gamma_{\mathrm{TT}}^{(hh)}|_{3\text{-point}} = \prod_{i=1}^{3} \int_0^\infty \frac{d\lambda_i^2}{2\pi} \rho_h(\lambda_i) I_{3\text{-point}}(p, \{\lambda_j\}), \quad (9)$$

for the diagram with graviton three-point vertices (second diagram in Fig. 1), and similarly for the other diagrams. The three spectral values relate to the three propagators in the diagram, and the function $I_{3\text{-point}}$ accounts for all tensor contractions and a remaining loop momentum integration. The latter integral can be performed analytically. In Eq. (9), we only need the spectral function Eq. (4) at $\vec{p} = 0$ due to Lorentz invariance. For the single-graviton delta peak, also the λ_i integrals in Eq. (9) can be performed straightforwardly, leading to closed analytic flows.

The graviton spectral function is obtained by integrating the flow Eq. (8). Here, we solve Eq. (8) without feeding back f_h on the right-hand side. This contribution is subleading and will be considered elsewhere.

Single-graviton peak.—We start with the flow of the single-graviton delta peak. Remarkably, our on-shell flows do not suffer from poles in the graviton propagator ($\mu = -1$) which are commonplace in off-shell studies. The three-graviton vertex, evaluated at vanishing momentum, provides the flow for Newton's coupling $G_N(k) = g(k)/k^2$ with an asymptotically safe UV fixed point

$$(g, \eta_h, \mu)|_* = (1.06, 0.96, -0.34). \qquad (10)$$

The scaling exponents $\theta = 2.49 \pm 3.17i$ compare well with those found in Euclidean studies. To connect the short-distance fixed point Eq. (10) with general relativity Eq. (1) at large distances, we impose the boundary conditions

$$(G_N(k), Z_h(k), k^2\mu(k))|_{k\to 0} = (G_N, 1, -2\Lambda), \quad (11)$$

where we have identified the infrared (IR) mass term with the cosmological constant in Eq. (1). Note that for normalizable spectral functions with $\int \lambda \rho(\lambda) d\lambda = 1$, the on-shell value of the wave function follows from this normalization. The on-shell choice $Z_h = 1$ is only possible as ρ_h cannot be normalized: $\int \lambda \rho_h(\lambda) d\lambda = \infty$ following from its scaling in the UV regime, see [25].
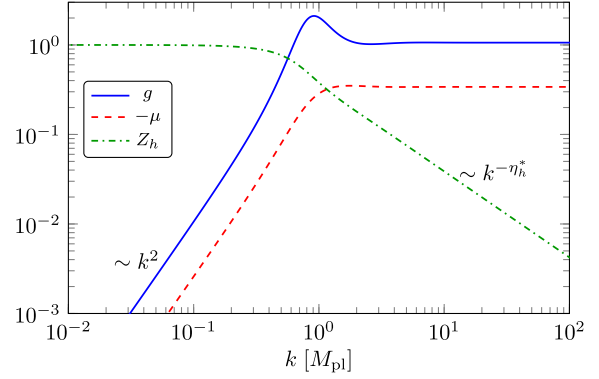
FIG. 2. UV-IR connecting trajectory showing the dimensionless Newton coupling g, the graviton mass parameter μ, and the graviton wave-function renormalization Z_h.

For now, we demand Λ to vanish. Besides being viable phenomenologically, it also ensures that the on-shell condition on a flat Minkowski background remains satisfied. The resulting RG trajectory for (g, Z_h, μ) is displayed in Fig. 2, with the Planck scale set to $M_{\mathrm{pl}}^2 = 1/G_N$. We observe that Z_h becomes a constant in the IR while it scales as $\sim k^{\eta_h}$ in the UV, whereas g and $-\mu$ scale $\sim k^2$ in the IR and settle at fixed points in the UV. The spike for g around the Planck scale can be traced back to the complex conjugate nature of the scaling exponents.

Multigraviton continuum.—The multigraviton continuum is found by integrating the flow Eq. (8) with Eq. (4) on the trajectory displayed in Fig. 2. Structurally, the flow is proportional to $\theta(\lambda^2 - 4m_h^2)$ with the largest contribution at the threshold. Consequently, the spectral function at λ is predominantly built from quantum fluctuations at $k \approx \lambda/(2\sqrt{1+\mu})$ which supports our approximation of dropping the multigraviton continuum f_h on the right-hand side of the flow. Our result for f_h is shown in Fig. 3. The function f_h approaches a constant below the Planck scale, and scales as $\sim \lambda^{\eta_h^* - 2}$ above the Planck scale. The spike near the Planck scale can be traced back to the complex conjugate scaling exponents, as was the case for g. Overall, the spectral function contains a massless delta peak and a positive multigraviton continuum, constant in the IR and with an asymptotically safe scaling in the UV. The same attributes were found in the recent reconstruction from Euclidean data [25].

The finite value of the spectral function in the IR implies the presence of a subleading logarithm in the propagator $\mathcal{G}_{hh} \sim p^{-2} - A_h \ln p^2 +$ subleading, as highlighted in the inset in Fig. 3. The coefficient A_h is universal (regulator independent) but gauge dependent [25,57]. It can be determined within effective theory, giving $A_h = 61/(60\pi) \approx 0.32$. Conversely, integrating the flow gives $A_h = 35/(9\sqrt{3}) - 11/(2\pi) \approx 0.49$. The difference is due to the neglected feedback of f_h, and serves as an indicator for subleading corrections. We conclude that our approximation does not
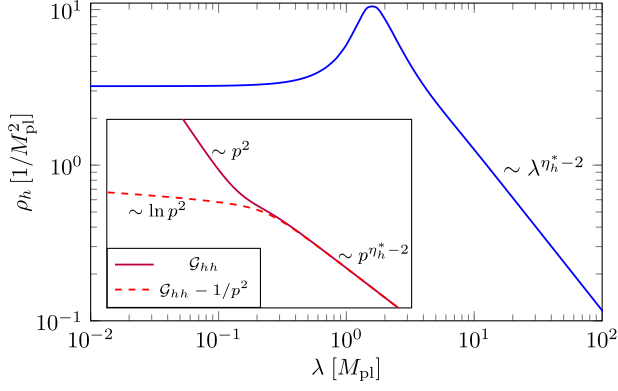
FIG. 3. The graviton spectral function. The inset shows the reconstructed Euclidean propagator (full line) and the subleading logarithm (dashed line).

affect the leading behavior of the propagator or global characteristics of the spectral function. We remark that the gauge dependence of the spectral function, which can be computed exactly in the IR via effective theory, is also present in the UV. Only the on-shell graviton delta peak is gauge independent.

With the spectral function and using Eq. (2), we have access to the propagator in the whole complex momentum plane. The real and imaginary parts of the propagator are depicted in Fig. 4, where we excluded the pole contribution in the real part. Both parts vanish for asymptotically large p. The real part displays a unique pole at vanishing p (not shown in Fig. 4), while the imaginary part shows a branch cut along the timelike axis.

Cosmological constant.—Next, we turn to Lorentzian quantum gravity with a nonvanishing cosmological constant. On de Sitter (dS) or anti–de Sitter (AdS) backgrounds, the classical graviton and ghost continue to be massless, and graviton vertices are deformed in comparison with flat backgrounds. Since alterations of the geometry are relevant for large spatial distances, we expect to find modifications of the spectral function at small spectral values. We continue to use flat backgrounds as above,

meaning that our setup at $\Lambda \neq 0$ becomes an off-shell expansion. For simplified trajectories

$$G_N(k) = \frac{g^*}{k^2 + g^* M_{\mathrm{pl}}^2}, \tag{12}$$

the spectral flows admit analytic solutions which facilitate the present qualitative discussion. In Eq. (12), g^* takes the role of a free parameter. Furthermore, we neglect the ghost contributions. The respective UV fixed point is given by

$$\mu^* = \frac{-g^*}{c_\mu + g^*}, \qquad \eta_h^* = \frac{2g^*}{2c_\eta + g^*}, \tag{13}$$

with $(c_\mu, c_\eta) = (1.77, 0.49)$ known analytically and provided in the Supplemental Material. Using $g^* = 1.06$ from Eq. (10), we find $\mu^* = -0.38$ and $\eta_h^* = 1.04$, both values being approximately 10% off, see Eq. (10). This indicates that the ghost contributions are indeed subleading.

The flow is readily integrated analytically with the IR boundary conditions (11),

$$Z_h(k) = \left(1 + \frac{1}{c_\eta \eta_h^*} \frac{k^2}{M_{\mathrm{pl}}^2}\right)^{-\frac{1}{2}\eta_h^*},$$

$$\mu(k) = \mu^* - \frac{2\Lambda}{k^2} + \frac{c_1 M_{\mathrm{pl}}^2 - 2\Lambda}{k^2}[Z_h(k)^{-c_2} - 1], \tag{14}$$

with $c_1 = 2.17g^*/(1.77 + g^*)$ and $c_2 = 0.45$ (further details including analytical expressions are given in the Supplemental Material).

Several comments are in order. For g^* taking real positive values, the graviton anomalous dimension ranges within $\eta_h^* \in (0, 2)$. We therefore have $Z_h \to 1$ in the IR, and $Z_h \to 0$ in the UV with a power law that mildly depends on g^*, reminiscent of the full solution for $\Lambda = 0$ (Fig. 2). The crossover sets in at $k^2/M_{\mathrm{pl}}^2 \approx c_\eta \eta_h^*$ which is close to but smaller than the Planck scale. Remarkably, the short distance mass parameter is constrained within the narrow range $\mu^* \in (-1, 0)$ and only takes negative values. From

FIG. 4. Real and imaginary part of the graviton propagator in the complex plane. The dashed line indicates the timelike axis.
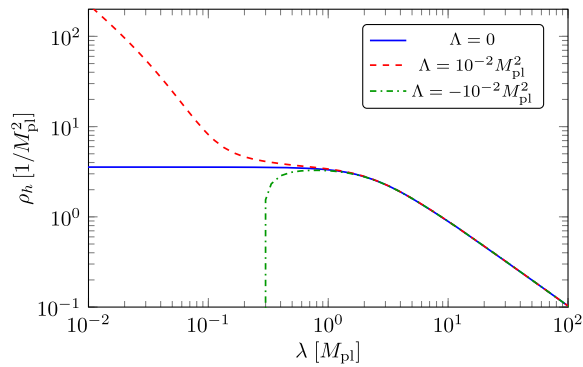
FIG. 5. Enhancement (or suppression) of the spectral function due to a positive (or negative) cosmological constant.

the explicit result Eq. (14), and also observing $c_2\eta_h^* < 1$, it is evident that the mass parameter $\mu(k)$ interpolates smoothly between μ^* in the UV and the cosmological constant $-2\Lambda/k^2$ in the IR. We conclude that Eqs. (12) and (14) are viable approximate solutions interpolating between an asymptotically safe fixed point and general relativity with a cosmological constant.

Following the same steps as before, we can now find the spectral function for $\Lambda \neq 0$ by integrating the flow Eq. (8) with Eq. (4) along the trajectories Eqs. (12) and (14). Our results are illustrated in Fig. 5. We observe that a positive or negative cosmological constant does not affect the spectral function for spectral values above $\lambda \gtrsim \sqrt{|8\Lambda|}$. For smaller spectral values, the geometry leaves an imprint. For AdS backgrounds, the cosmological constant acts like a mass term which leads to a suppression. Conversely, the spectral function is enhanced for dS backgrounds because $\Lambda > 0$ acts like a negative mass-squared term.

The off-shell effects due to the cosmological constant become even more pronounced if the ghost contributions are retained. The ghost remains on-shell at k^2 compared to the off-shell graviton at $m_h^2 = k^2(1 + \mu)$. We find that for AdS backgrounds (at $\mu = 3$), off-shell gravitons can directly scatter into the on-shell multighost continuum and the flow of f_h diverges, while it stays finite for dS backgrounds. In this off-shell computation, the flat Minkowski background bears similarities to an *external* electric or magnetic field in QED. External backgrounds or boundary conditions can introduce driving forces or friction that constantly feed or suppress scattering processes, which then destroy unitarity much like in open quantum systems. This analogy allows for a heuristic interpretation of the AdS singularity in the flow: there the off-shell background serves as a driving force for graviton scattering processes. We expect that full on-shell AdS flows with ghost contributions remain finite. Then, graviton and ghost are both on-shell massless, and it is the off-shell shift of mass scales that triggers the divergence.

Discussion and conclusion.—We have put forward the first direct computation of the graviton spectral function in

quantum gravity. The spectral function shows a massless one-graviton peak and a positive multigraviton scattering continuum (Fig. 3), interpolating between a constant part for small and an asymptotically safe scaling regime for large spectral values. While the spectral function can always be defined as the imaginary part of the retarded propagator Eq. (3), the KL representation Eq. (2) only holds if the propagator has no poles or cuts in the complex upper half plane. Therefore, it is quite remarkable that the graviton spectral function and propagator *indeed* obey the KL representation Eq. (2) with a positive spectral function and no ghost or tachyonic instabilities. The absence of the latter instabilities is crucial for the unitarity of the theory. This noteworthy result should be contrasted with the unclear situation in non-Abelian gauge theories where a similar understanding has not yet been achieved [35,36,58–62].

On the technical side, and to ensure that the KL representation Eq. (2) is not inadvertently spoiled by the momentum cutoff, the spectral flow necessitates *spectral* regulators which do not introduce cuts and poles in the complex upper half plane. In our study, we have explicitly observed the absence of the latter, which therefore guarantees a spectral representation for all scales. Further, we have advocated the unique Lorentz-invariant *spectral* cutoff Eq. (5), at the expense of an additional regularization (6). The latter can be avoided by using spatial cutoffs, though at the price of breaking Lorentz invariance. Still, the corresponding flows are linked to the CS spectral flow in well-defined limits, and offer avenues for systematic error estimates.

Finally, we note that our findings open a door to investigate scattering amplitudes and unitarity of fully quantized gravity [25,56,63–66]. The key building blocks are the timelike graviton propagator obtained here (Fig. 4), and the corresponding spectral functions for scattering vertices. Extracting vertices from Eqs. (6) and (8) is in reach, albeit technically more demanding than extracting propagators. We thus look forward to direct tests of unitarity in asymptotically safe gravity.

[1] A. Ashtekar, M. Reuter, and C. Rovelli, arXiv:1408.4336.
[2] S. Weinberg, *General Relativity: An Einstein Centenary Survey*, edited by S. W. Hawking and W. Israel (Cambridge University Press Cambridge, England, 1979), 790.
[3] M. Reuter, Phys. Rev. D **57**, 971 (1998).

[4] D. F. Litim, Phil. Trans. R. Soc. A **369,** 2759 (2011).
[5] A. Bonanno and F. Saueressig, C.R. Phys. **18,** 254 (2017).
[6] A. Eichhorn, Front. Astron. Space Sci. **5,** 47 (2019).
[7] A. D. Pereira, arXiv:1904.07042.
[8] M. Reuter and F. Saueressig, *Quantum Gravity and the Functional Renormalization Group* (Cambridge University Press, Cambridge, England, 2019).
[9] M. Reichert, *Proc. Sci.*, Modave2019 (2020) 005.
[10] A. Platania, Front. Phys. **8,** 188 (2020).
[11] A. Bonanno, A. Eichhorn, H. Gies, J. M. Pawlowski, R. Percacci, M. Reuter, F. Saueressig, and G. P. Vacca, Front. Phys. **8,** 269 (2020).
[12] N. Dupuis, L. Canet, A. Eichhorn, W. Metzner, J. M. Pawlowski, M. Tissier, and N. Wschebor, Phys. Rep. **910,** 1 (2021).
[13] J. M. Pawlowski and M. Reichert, Front. Phys. **8,** 527 (2020).
[14] J. F. Donoghue, Front. Phys. **8,** 56 (2020).
[15] E. Manrique, S. Rechenberger, and F. Saueressig, Phys. Rev. Lett. **106,** 251302 (2011).
[16] S. Rechenberger and F. Saueressig, J. High Energy Phys. 03 (2013) 010.
[17] M. Demmel and A. Nink, Phys. Rev. D **92,** 104013 (2015).
[18] J. Biemans, A. Platania, and F. Saueressig, Phys. Rev. D **95,** 086013 (2017).
[19] W. B. Houthoff, A. Kurov, and F. Saueressig, Eur. Phys. J. C **77,** 491 (2017).
[20] C. Wetterich, Phys. Lett. B **773,** 6 (2017).
[21] B. Knorr, Phys. Lett. B **792,** 142 (2019).
[22] A. Baldazzi, R. Percacci, and V. Skrinjar, Classical Quantum Gravity **36,** 105008 (2019).
[23] S. Nagy, K. Sailer, and I. Steib, Classical Quantum Gravity **36,** 155004 (2019).
[24] A. Eichhorn, A. Platania, and M. Schiffer, Phys. Rev. D **102,** 026007 (2020).
[25] A. Bonanno, T. Denz, J. M. Pawlowski, and M. Reichert, SciPost Phys. **12,** 001 (2022).
[26] J. Ambjorn and R. Loll, Nucl. Phys. **B536,** 407 (1998).
[27] J. Ambjorn, J. Jurkiewicz, and R. Loll, Phys. Rev. Lett. **85,** 924 (2000).
[28] J. Ambjorn, J. Jurkiewicz, and R. Loll, Nucl. Phys. **B610,** 347 (2001).
[29] J. Engle, R. Pereira, and C. Rovelli, Phys. Rev. Lett. **99,** 161301 (2007).
[30] L. Freidel and K. Krasnov, Classical Quantum Gravity **25,** 125018 (2008).
[31] J. Feldbrugge, J.-L. Lehners, and N. Turok, Phys. Rev. D **95,** 103508 (2017).
[32] S. K. Asante, B. Dittrich, and J. Padua-Arguelles, Classical Quantum Gravity **38,** 195002 (2021).
[33] G. Kallen, Helv. Phys. Acta **25,** 417 (1952).
[34] H. Lehmann, Nuovo Cimento **11,** 342 (1954).
[35] A. K. Cyrol, J. M. Pawlowski, A. Rothkopf, and N. Wink, SciPost Phys. **5,** 065 (2018).
[36] J. Horak, J. Papavassiliou, J. M. Pawlowski, and N. Wink, Phys. Rev. D **104,** 074017 (2021).
[37] J. Horak, J. M. Pawlowski, and N. Wink, Phys. Rev. D **102,** 125016 (2020).
[38] K. Symanzik, Commun. Math. Phys. **18,** 227 (1970).
[39] C. Wetterich, Phys. Lett. B **301,** 90 (1993).
[40] See Supplemental Material at http://link.aps.org/supplemental/10.1103/PhysRevLett.130.081501 for more details on the derivation and use of the spectral flow equation, including a detailed analytic approximation, which includes Refs. [41–53].
[41] T. Denz, A. Held, J. M. Pawlowski, and A. Rodigast (to be published).
[42] M. Q. Huber, A. K. Cyrol, and J. M. Pawlowski, Comput. Phys. Commun. **248,** 107058 (2020).
[43] M. Q. Huber and A. K. Cyrol, DoFun GitHub Repository (2019), https://github.com/markusqh/DoFun.
[44] J. M. Martín-García, Comput. Phys. Commun. **179,** 597 (2008).
[45] D. Brizuela, J. M. Martin-Garcia, and G. A. Mena Marugan, Gen. Relativ. Gravit. **41,** 2415 (2009).
[46] A. K. Cyrol, M. Mitter, and N. Strodthoff, Comput. Phys. Commun. **C219,** 346 (2017).
[47] A. K. Cyrol, M. Mitter, J. M. Pawlowski, and N. Strodthoff, FormTracer GitHub Repository (2016), https://github.com/FormTracer/FormTracer.
[48] F. Feng and R. Mertig, arXiv:1212.3522.
[49] B. Ruijl, T. Ueda, and J. Vermaseren, arXiv:1707.06453.
[50] T. Huber and D. Maitre, Comput. Phys. Commun. **175,** 122 (2006).
[51] B. Knorr and M. Schiffer, Universe **7,** 216 (2021).
[52] D. F. Litim, Phys. Lett. B **486,** 92 (2000).
[53] D. F. Litim, Phys. Rev. D **64,** 105007 (2001).
[54] J. Braun, Y.-r. Chen, W.-j. Fu, A. Geißel, J. Horak, C. Huang, F. Ihssen, J. M. Pawlowski, M. Reichert, F. Rennecke, Y.-y. Tan, S. Töpfel, J. Wessely, and N. Wink, arXiv:2206.10232.
[55] N. Christiansen, B. Knorr, J. Meibohm, J. M. Pawlowski, and M. Reichert, Phys. Rev. D **92,** 121501(R) (2015).
[56] T. Denz, J. M. Pawlowski, and M. Reichert, Eur. Phys. J. C **78,** 336 (2018).
[57] R. E. Kallosh, O. V. Tarasov, and I. V. Tyutin, Nucl. Phys. **B137,** 145 (1978).
[58] S. W. Li, P. Lowdon, O. Oliveira, and P. J. Silva, Phys. Lett. B **803,** 135329 (2020).
[59] D. Binosi and R.-A. Tripolt, Phys. Lett. B **801,** 135171 (2020).
[60] Y. Hayashi and K.-I. Kondo, Phys. Rev. D **103,** L111504 (2021).
[61] Y. Hayashi and K.-I. Kondo, Phys. Rev. D **104,** 074024 (2021).
[62] Y. Kluth, D. F. Litim, and M. Reichert, Phys. Rev. D **107,** 025011 (2023).
[63] B. Knorr, C. Ripken, and F. Saueressig, Classical Quantum Gravity **36,** 234001 (2019).
[64] T. Draper, B. Knorr, C. Ripken, and F. Saueressig, Phys. Rev. Lett. **125,** 181301 (2020).
[65] T. Draper, B. Knorr, C. Ripken, and F. Saueressig, J. High Energy Phys. 11 (2020) 136.
[66] A. Platania and C. Wetterich, Phys. Lett. B **811,** 135911 (2020).